Plasticity of Meiotic Recombination Rates in Response to Temperature in *Arabidopsis*

Andrew Lloyd,*[,1,2] Chris Morgan,[†,‡,2] F. Chris H. Franklin,[‡] and Kirsten Bomblies[†,1]

*Institut Jean-Pierre Bourgin, Institut National de la Recherche Agronomique, AgroParisTech, Centre National de la Recherche Scientifique, Université Paris-Saclay, 78000 Versailles, France, [†]Department of Cell and Developmental Biology, John Innes Centre, Norwich, NR4 7UH, United Kingdom, and [‡]School of Biosciences, University of Birmingham, Edgbaston, B15 2TT, United Kingdom

ORCID IDs: 0000-0001-7871-6621 (A.L.); 0000-0003-3507-722X (F.C.H.F.); 0000-0002-2434-3863 (K.B.)

ABSTRACT Meiotic recombination shuffles genetic information from sexual species into gametes to create novel combinations in offspring. Thus, recombination is an important factor in inheritance, adaptation, and responses to selection. However, recombination is not a static parameter; meiotic recombination rate is sensitive to variation in the environment, especially temperature. That recombination rates change in response to both increases and decreases in temperature was reported in *Drosophila* a century ago, and since then in several other species. But it is still unclear what the underlying mechanism is, and whether low- and high-temperature effects are mechanistically equivalent. Here, we show that, as in *Drosophila*, both high and low temperatures increase meiotic crossovers in *Arabidopsis thaliana*. We show that, from a nadir at 18°, both lower and higher temperatures increase recombination through additional class I (interfering) crossovers. However, the increase in crossovers at high and low temperatures appears to be mechanistically at least somewhat distinct, as they differ in their association with the DNA repair protein MLH1. We also find that, in contrast to what has been reported in barley, synaptonemal complex length is negatively correlated with temperature; thus, an increase in chromosome axis length may account for increased crossovers at low temperature in *A. thaliana*, but cannot explain the increased crossovers observed at high temperature. The plasticity of recombination has important implications for evolution and breeding, and also for the interpretation of observations of recombination rate variation among natural populations.

KEYWORDS recombination; crossover plasticity; recombination rate; temperature; meiosis

THE vast majority of eukaryotes rely on meiosis to produce gametes. One important process within meiosis is the crossing-over of homologous chromosomes, which in most eukaryotes is essential for stable chromosome segregation (Zickler and Kleckner 1999). Recombination also shuffles the genetic complements of the two parents of an individual and is thus important in generating novel genetic combinations in gametes and ultimately offspring. The extent and pattern of genetic reshuffling via homologous recombination has important implications for evolution and adaptation, as well as population genetics and breeding (*e.g.*, Barton 1995; Charlesworth and Barton 1996; Otto 2009; Campos *et al.* 2015). Recombination is not a static parameter between, or even within, taxa. Meiotic recombination rate is known to be sensitive to a variety of environmental factors, particularly temperature (Plough 1917; Elliott 1955; De Storme and Geelen 2014; Bomblies *et al.* 2015; Modliszewski and Copenhaver 2015; Phillips *et al.* 2015). Extreme temperatures can cause meiotic recombination to fail outright due to structural disruptions of, *e.g.*, the spindle, the chromosome axes, or the synaptonemal complex (SC) (Bilgir *et al.* 2013; Bomblies *et al.* 2015; Morgan *et al.* 2017). We refer to the temperatures at which such defects become cytologically evident as "failure thresholds." Less-extreme temperature fluctuations that do not cause outright failures can nevertheless affect the genome-wide recombination rate in diverse taxa (Plough 1917; Elliott 1955; De Storme and Geelen 2014; Bomblies

doi: https://doi.org/10.1534/genetics.117.300588
Manuscript received December 5, 2017; accepted for publication February 2, 2018; published Early Online February 9, 2018.
Available freely online through the author-supported open access option.
Supplemental material is available online at www.genetics.org/lookup/suppl/doi:10.1534/genetics.117.300588/-/DC1.
[1]These authors contributed equally to this work.
[2]Corresponding authors: Institut Jean-Pierre Bourgin, INRA, AgroParisTech, CNRS, Université Paris-Saclay, RD10, 78000 Versailles, France. E-mail: andrewhmlloyd@gmail.com; and John Innes Centre, Norwich Research Park, Colney Lane, Norwich, NR4 7UH, United Kingdom. E-mail: Kirsten.Bomblies@jic.ac.uk

et al. 2015; Modliszewski and Copenhaver 2015; Phillips *et al.* 2015). Understanding the nature and strength of these effects has important implications for better understanding and predicting inheritance and evolution, especially in a time of climate change, and also for managing breeding programs. Understanding the effect of temperature on recombination also provides opportunities to manipulate recombination in a targeted and reversible way (*e.g.*, Phillips *et al.* 2015).

That both temperature increases and decreases can affect meiotic recombination rates has been recognized for 100 years (Plough 1917). The first investigation into the effect of temperature on meiotic recombination rate suggested a U-shaped response in *Drosophila* (Plough 1917; Smith 1936), meaning that midrange temperatures (which at least in the case of *Drosophila* correspond to common rearing temperatures) have the lowest recombination rate, and both increases and decreases in rearing temperature are associated with elevated recombination. Since the original discoveries, a variety of trends have been reported, including no effect, increases with increasing temperature, and decreases with increasing temperature (Stern 1926; Elliott 1955; Jensen 1981; Francis *et al.* 2007; Phillips *et al.* 2015), reviewed in Bomblies *et al.* (2015). We and others have previously suggested that, while there may well be biological differences among taxa, distinct reported trends can also result from differences in experimental design (Wilson 1959; Bomblies *et al.* 2015), *e.g.*, from only sampling a subsection of the relevant temperature range, or by including temperatures beyond the meiotic failure limits where recombination declines sharply. Many species appear to have U-shaped curves (Wilson 1959; Bomblies *et al.* 2015), but it has remained unknown whether the low- and high-temperature effects are mechanistically distinct.

An important aspect of understanding the effects of temperature on recombination is to know what type of crossovers are responsible, as this has important implications for the patterning that may result. Crossovers come in two major classes. Class I crossovers represent the majority of crossovers in most species (Lynn *et al.* 2007). These crossovers rely on a class of proteins called ZMM (which stands for the yeast meiotic genes *Zip1/Zip2/Zip3/Zip4*, *Msh3/Msh5*, *Mer3*) proteins (Börner *et al.* 2004; Lynn *et al.* 2007; Mercier *et al.* 2014) and are subject to crossover interference. Crossover interference deters crossovers from forming in close proximity, and thus causes recombination events to be more widely spaced than expected if they occurred randomly (Berchowitz and Copenhaver 2010). A second class are called the class II crossovers. These occur through a variety of pathways, but share the important property that they are not subject to crossover interference and can be spaced randomly (Lynn *et al.* 2007; Higgins *et al.* 2012). In most species, it is not known whether temperature affects one or the other type of crossover preferentially. In barley, where temperature causes a change in the positioning of crossovers to more proximal locations (Higgins *et al.* 2012; Phillips *et al.* 2015), immunological staining suggests that class I crossovers are affected. In yeast, temperature also has effects on ZMM-dependent (class I) crossover designation (Börner *et al.* 2004). Whether temperature effects operate primarily through altering class I or class II crossovers has implications for how crossover positioning and spacing will be affected.

In *Arabidopsis thaliana*, a positive relationship between temperatures from 19 to 28° and male meiotic recombination was previously described (Francis *et al.* 2007). However, this temperature range represents only the upper portion of the viable range; *A. thaliana* can also flower and produce seeds at much lower temperatures. Here, we study the effect of temperature on male meiotic recombination in *A. thaliana* across a wider temperature range than has been previously examined. We test whether lower and higher temperatures affect class I and/or class II crossover frequency, and also explore whether changes in the length of the chromosome axes and SC might suffice to explain the effects of temperature on recombination rate in *A. thaliana*.

Materials and Methods

Plant growth

Col-0 plants were grown under long-day growth conditions (16 hr day at 19–21°/8 hr night at 15°) until the primary inflorescence began to emerge from the rosette. Plants were then transferred to a range of small, constant temperature, long-day growth chambers at the experimental temperatures (5–30°). For cytology, plants were grown to the same developmental age and height after flowering, and then transferred to growth chambers at 8, 18, or 28° for 1 week before material was collected to make slides. As the duration of meiosis has previously been demonstrated to last 33 hr at 18.5° (Armstrong *et al.* 2003), 1 week was chosen to be long enough to complete meiosis at each temperature without causing a significant impact on the developmental trajectory of the plants.

For flow cytometry, after transferring to constant temperature chambers, plants were grown until at least five or six inflorescences had emerged and flowered, thus providing sufficient pollen for flow cytometric analyses: 28°; 23°, 1 week, 18°, 2 weeks; 13°, 3 weeks; and 8°, 5 weeks.

Seed set

Seed set was quantified as seeds per silique. For each temperature, seeds were counted for 3–10 siliques for each of three or four biological replicates (plants). All siliques originated from the primary inflorescence.

Pollen viability

Method 1: For each temperature, pollen viability was determined by Alexander staining for two to four plants. For each plant ~200 pollen grains were counted. All flowers originated from the primary inflorescence. Pollen viabilities reported are the means of the biological replicates for each temperature.

Method 2: When analyzing flow cytometry data, single pollen grains were subdivided into two populations (viable and nonviable) based on side scatter (SSC)/forward scatter

(FSC) (Supplemental Material, Figure S9, A–C in File S1). To confirm their composition, the two populations were sorted using a MoFlo ASTRIOS (Beckman, Fullerton, CA), stained using Alexander's stain (10%), and viewed under a light microscope (Figure S9, D–G in File S1). While the presumed nonviable population consisted solely of nonviable pollen grains, the presumed viable population contained both viable and nonviable pollen grains (Figure S9, D–H in File S1). This method therefore provides an output proportional to pollen viability, but systematically overestimates pollen viability.

Pollen fluorescence detection

For each Fluorescent Tagged Line (FTL) and each temperature, flowers were collected for a minimum of three pools of three plants, each pool representing one biological replicate. Pollen was isolated and analyzed as described in Yelina *et al.* (2013). An LSR Fortessa (BD Biosciences) was used for analysis, with 440, 488, and 561 nm lasers and 470/20, 530/30, and 582/15 bandpass filters used for detection of enhanced cyan fluorescent protein (eCFP), enhanced yellow fluorescent protein (eYFP), and dsRED, respectively. A standard run consisted of 50,000–100,000 pollen grains for each biological replicate.

Analysis of flow cytometry data

Single viable pollen grains were first sorted into subsets based on size and granularity parameters, FSC and SSC, respectively (Figure S9, A–C in File S1). Due to loss of fluorescent signal (but not loss of the respective transgene) in a significant proportion of pollen grains, a gating strategy was first used to eliminate potential false negatives prior to recombination analysis. Using this strategy, pollen grains were first subset based on detection of the "control" fluorophore and then scored for recombination based on the presence/absence of the "diagnostic" fluorophore (Figure S10, A–D in File S1). The fluorophore used as the control had the less-stable signal and the diagnostic fluorophore had the more-stable signal. This ensured that, for pollen grains used in analysis, loss of signal was due to recombination (*i.e.*, true absence of the transgene) rather than a false negative loss of signal (Figure S10, E and F in File S1).

A similar approach using two diagnostic fluorophores was used to detect double crossovers (DCOs, Figure S11 in File S1). Although reciprocal results (*e.g.*, $eCFP^{+}/eYFP^{+/-}$ *vs.* $eYFP^{+}/eCFP^{+/-}$) gave relatively consistent recombination frequencies (Figures S10 and S11 in File S1), there were some discrepancies. To assess which fluorophore detection regime gave the most accurate results, we exploited the fact that for intervals Ia and Ib: $SCO_{Ia} + SCO_{Ib} = SCO_{Iab} + 2{*}DCO_{Iab}$. For each regime, we assessed the concordance between ($SCO_{Ia} + SCO_{Ib}$) and ($SCO_{Iab} + 2{*}DCO_{Iab}$) and used the regime that gave the most concordant results in all further analyses (*e.g.*, Figure S12 in File S1).

Beam-film modeling and analysis

Best-fit parameters for the FTL intervals on chromosomes 3 and 5 were determined using MADpatterns (White *et al.* 2017) and custom perl scripts, using an approach based on that described in Zhang *et al.* (2014). Parameter value ranges [Smax (the crossover designation driving force): 1–8.5; L (the proportion of the chromosome over which interference propagates, *i.e.*, the proportion of the chromosome over which stress is relieved): 0.7–1; T2 Prob (the proportion of potential crossover sites that develop into noninterfering class II crossovers): 0.0025–0.011; cL: 0.9–1.6; and cR: 0.9–1.6) were chosen based on parameter values described in Zhang *et al.* (2014) and comparison of *ad hoc* simulations with analysis of a large *Arabidopsis* whole-genome recombination data set described in Basu-Roy *et al.* (2013). Final best-fit parameters for the FTL intervals were identified by comparing simulated data with the experimental FTL data.

Crossovers were simulated using a range of parameter combinations (50,000 bivalents per parameter set): parameters Smax, L, T2 Prob, cL, and cR were varied, while parameters B, Bsmax, A, and M were set at appropriate default values (Zhang *et al.* 2014). The number of precursor sites (N) was calculated based on the total number of double-strand breaks (DSBs) expected per meiosis in *Arabidopsis* (~250) multiplied by the proportion of the genome length contributed by the chromosome being simulated. Appropriate values for the position and strength of recombination "black holes" (Bs, Be, and Bd)—corresponding to recombination-suppressed centromeres—were chosen based on the analysis of experimental data in Basu-Roy *et al.* (2013). Simulated chromosomes were analyzed for crossover distribution and coefficient of coincidence (CoC) in the regions of the simulated chromosomes corresponding to the respective FTL intervals using the procedure outlined in White *et al.* (2017). For each parameter set, the simulated recombination frequencies and CoC values were compared to values derived from the experimental FTL data. Importantly, the experimental data are gamete data, while the MADpatterns program simulates (and outputs) bivalent data (*i.e.*, for a chromosome pair). Therefore, all simulated bivalent crossover frequencies were halved to convert to gamete crossover frequencies. Parameter sets were then ranked, first based on the difference between the simulated and experimentally determined CoC values [$Score_{CoC} = (CoC_{sim} - CoC_{FTL})^2$] and second based on the difference between the observed FTL recombination frequencies and the simulated (gamete) recombination frequencies of the two intervals [$Score_{RF} = abs\{log2(RFI1_{sim}/RFI1_{FTL})\} + abs\{log2(RFI2_{sim}/RFI2_{FTL})\}$]. The final parameter values chosen (Table 1) were those with the lowest rank-sum. At least three rounds of analysis, with progressively smaller step sizes between values, were used to arrive at the final parameter values.

Finally, we modeled the effects on the CoC of increased crossovers caused by changes in a single parameter of the MADpatterns program (either Smax, L, or T2 Prob). For each parameter, the value was adjusted until a ~13% increase in crossovers had been achieved (*i.e.*, the average increase in crossovers observed between 18° and temperature extremes; Table 1), and the changes in CoC predicted for each

Table 1 Best-fit parameters for chromosomes 3 and 5

Chr	*N*	B	E[a]	Bs	Be	Bd	Smax	Bsmax	A	L	cL	cR	M	T2prob
5	56	1	0.6	0.4	0.5	0.01	4.5 (15)	1	1	1 (0.54)	0.8	1.05	1	0.0095 (0.0155)
3	49	1	0.6	0.5	0.65	0.01	1 (2.03)	1	1	0.9 (0.641)	1.5	1.5	1	0.01 (0.0162)

Values in brackets are those used to achieve a 13% increase in crossovers. Chr, chromosome; N = number of precursor sites. Model parameters are defined as follows (see White et al. 2017; Zhang et al. 2014): B= Precursor distribution among bivalents (0 = Poisson, 1 = constant), E= Precursor distribution along bivalents (0 = random, 1 = even), Bs = Black hole (centromere) start position, Be= Black hole (centromere) end position, Bd= Precursor density within black hole relative to rest of bivalent, Smax= Designation driving force (Progressively increased to Smax during simulation), Bsmax= Distribution of Smax among bivalents. (0 = Poisson, 1 = constant), A= Determines distribution of precursor sensitivities. Default A = 1. L= Proportion of bivalent over which the interference signal propagates. cL / cR: End effects on interference (Left/Right) where 0 = unclamped – behaves as if there was a CO at the end of the chromosome and 1 = clamped - behaves as if there was not a CO at the end of the chromosome, M= Efficiency with which CO-designation matures to eventual CO, T2prob= Probability of a precursor site becoming a class II CO.

[a] Whole chromosomes were simulated, with best-fit parameters based on Fluorescent Tagged Line-derived crossover and coefficient of coincidence values.

parameter change were then compared to those observed experimentally (Figure 2).

Cytological procedures

Immunolocalization slides using fresh material and DAPI-stained spreads using acid-fixed material were prepared as described previously (Caryl *et al.* 2000; Armstrong *et al.* 2002). The following antibodies and dilutions were used: anti-AtMLH1 (rat, 1/200 dilution) (Higgins *et al.* 2005), anti-AtHEI10 (rat, 1/200 dilution and rabbit, 1/200 dilution) (Lambing *et al.* 2015), anti-AtZYP1 (rabbit, 1/500 dilution and guinea pig, 1/500 dilution) (Higgins *et al.* 2005), FITC anti-guinea pig (1/100; Abcam), alexa-fluor 488 anti-rat (1/500; ThermoFisher), alexa-fluor 594 anti-rabbit (1/500; ThermoFisher), alexa-fluor 555 anti-rat (1/800; Abcam), and alexa-fluor 647 anti-rabbit (1/800; Abcam). Epifluorescence microscopy was carried out using a Nikon 90i Fluorescence Microscope (Nikon, Garden City, NY) and image capture, analysis, and processing were conducted using NIS-Elements software (Nikon). Structured illumination microscopy was carried out using a Zeiss Elyra PS1 and image reconstruction and channel-alignment were carried out using ZEN black software (Zeiss [Carl Zeiss], Thornwood, NY). SC length measurements were made by measuring total SC length in three dimensions using the simple neurite tracer plugin to ImageJ with Z-stacked images of pachytene nuclei stained for ZYP1 (Longair *et al.* 2011). Measurements were only taken from cells in which five complete bivalents could be measured to ensure that cells were fully synapsed, and the five bivalent lengths were combined to give a total SC length for each cell. MLH1 and HEI10 foci were identified as bright, round foci that overlapped with the SC in the *x*, *y*, and *z* planes and were observed in late pachytene/early diplotene cells that were identified as either being fully synapsed or mostly synapsed with some small regions of SC disassembly, respectively. Note that HEI10 and MLH1 foci numbers in *Arabidopsis* have previously been shown to remain constant from late pachytene through diplotene (Chelysheva *et al.* 2012). Mann–Whitney *U*-tests were used to compare MLH1 and HEI10 foci counts and total SC lengths as described previously (Ziolkowski *et al.* 2017). This was appropriate as bulked anthers from multiple plants exposed to the same temperature treatment were used when making each immunolocalization slide and therefore each cell was treated as an independent observation.

Data availability

The authors state that all data necessary for confirming the conclusions presented in the article are represented fully within the article.

Results

Crossover rates in Arabidopsis are lowest in the middle of the fertile temperature range

We measured recombination both in meiocytes and in gametophytes. In the latter, recombination rate estimates can be confounded because: (1) recombination declines sharply due to structural failures when temperatures exceed failure thresholds, thus a biased view can arise if temperatures past the failure points are included, and/or (2) estimates can be biased due to failures in later stages of gametophyte development. Both sources of bias can be averted at least to some extent by avoiding temperatures that cause a decline in fertility. Thus, we first estimated the informative temperature range for *A. thaliana* by measuring seed set and pollen viability at temperatures from 5 to 30°. At the high end, seed set dropped significantly from 28 to 30° (Figure S1 in File S1). At 8°, seed set was no different from seed set at moderate temperatures (18°, $P = 1$ and 23°, $P = 1$; Student's *t*-test, Bonferroni corrected); however, there was no seed set at 5° (Figure S1 in File S1). The latter is consistent with previously observed postmeiotic defects following 4–5° Cold stress (De Storme *et al.* 2012). Therefore, for our purposes, we defined the "fertile range" of *A. thaliana* in our conditions as 8–28° and focused on this range to assay recombination. Within this temperature range there was no significant decrease in pollen viability at temperature extremes, although variance increased at higher temperature (Figure S2 in File S1). We also ascertained that we had not exceeded failure thresholds using cytological observations. In plants exposed to 8, 18, or 28° for 1-week synapsis, crossover formation and chromosomal segregation proceeded without appreciable errors in male meiocytes (Figure S3 in File S1), and at neither temperature extreme were obvious differences evident relative to 18°.

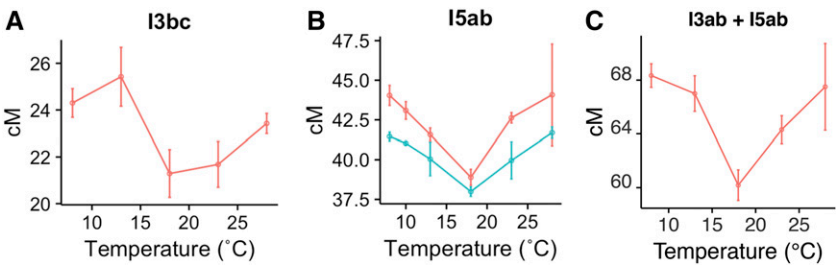

Figure 1 Meiotic recombination has a U-shaped response to temperature in *Arabidopsis*. Data from intervals I3bc and I5ab demonstrate a U-shaped response in recombination rate to temperature (A and B). For interval I5ab (B), the same trend is observed when plants have different numbers of secondary bolts and branches across the temperature range (red), or if all plants are harvested when they have 5five to six inflorescences (blue). The combined genetic length of intervals I3bc and I5ab is shown in (C). Error bars indicate 95% C.I.s.

To initially score recombination rates at different temperatures in high throughput, we capitalized on a previously developed transgenic tool that uses fluorescent markers to score male meiotic crossovers in pollen grains (Francis *et al.* 2007). We scored male crossover frequency in FTLs that flank two pairs of adjacent intervals on chromosome 3 (I3b and I3c) and chromosome 5 (I5a and I5b). While the FTL loci showed subtle differences in the responses at different temperatures (Figure 1 and Figures S4 and S5 in File S1), the overall shapes of the I3bc and I5ab distributions were not significantly different after normalizing for the different sizes of the intervals ($P = 0.873$, two-sample Kolmogorov–Smirnov test). Both pairs of intervals followed the same general trend with a minimum recombination rate at ~18°, and higher frequencies at both higher and lower temperatures (Figures S4 and S5 in File S1). The combined genetic length of the four intervals shows a clear U-shaped trend of recombination rates across the temperature range (Figure 1C). Using a Mann–Whitney–Wilcoxon Rank Test (unpaired Wilcoxon test) on combined data from the four intervals, we found that crossover rates were significantly lower (10–15%) at 18°, the center of the fertile temperature range, than at either 8 or 28° ($P = 7.76e^{-6}$ and $P = 2.22e^{-5}$, respectively). The upper half of the trend recapitulates previous findings in *A. thaliana* (assayed with markers on a different chromosome) of a positive trend from 19 to 28° (Francis *et al.* 2007). Since recombination rates can also be sensitive to developmental age (Francis *et al.* 2007), we tested whether this trend was merely a consequence of differences in overall development at the different temperatures (Figures 1B and Figure S6 in File S1). By assaying only plants at comparable developmental stages, *i.e.*, all plants with five to six inflorescences (Figure S6B in File S1), we showed that the increase in recombination rate at lower as well as higher temperatures is still evident. This indicates that *A. thaliana*, like *Drosophila* and several other species (Bomblies *et al.* 2015), has a U-shaped relationship between temperature and recombination rate.

Modeling predicts that increased crossovers occur via the class I pathway

We next explored which crossover pathways might be affected. In *A. thaliana*, the majority (85%) of crossovers are class I crossovers; these rely absolutely on a group of proteins called the ZMM proteins and are subject to crossover interference, which prevents crossovers occurring in close proximity (Mercier *et al.* 2005; Chelysheva *et al.* 2007, 2012; Higgins *et al.* 2008b). The remaining crossovers are collectively referred to as class II crossovers; these occur via several pathways and are not sensitive to crossover interference (Berchowitz *et al.* 2007; Higgins *et al.* 2008a). When measured genetically (as here), the CoC—the number of DCOs observed divided by the number expected in a given pair of intervals based on the single crossover rates—can provide insight into the relative contributions of the class I and class II crossover pathways (CoC should increase if additional crossovers are primarily class II noninterfering crossovers). For both pairs of intervals (I3b/I3c and I5a/I5b), we calculated CoC across the temperature range and observed no change, or a slight decrease in CoC at temperature extremes. This observation indicates that crossovers do not become noticeably more likely to occur near one another at higher or lower temperatures, suggesting that the increase in recombination rates may primarily involve class I (interfering) rather than class II crossovers (Figure 2, A and B).

We further tested this idea by simulating crossover patterning under the beam-film model, a leading model of crossover designation and interference (White *et al.* 2017). The beam-film model proposes a mechanical basis of crossover designation. Under this model, redistribution of mechanical stress along the chromosomes is the basis of crossover interference. Crossovers occur at precursor sites (*i.e.*, meiotic DSBs) in regions of high stress and locally relieve stress, preventing the formation additional crossovers nearby. Three important parameters of the beam-film model are Smax, L, and T2prob. Changes in these parameters affect the crossover frequency and the CoC predicted by the model. We determined the best-fit parameters for the intervals I5ab and I3bc in male meiosis (Table 1) using the experimental FTL data and a previously published large recombination data set (Basu-Roy *et al.* 2013). We then adjusted single-parameter values (Table 1) to model an increase in crossovers equivalent to that observed at higher and lower temperatures. We compared the observed CoC to the changes predicted by the beam-film model under different parameter values. When extra crossovers were simulated to occur via the class I (interfering) pathway, the predicted effects on CoC were consistent with our observations (Figure 2C, Smax and Figure 2D, Smax and L), but when extra crossovers were simulated to occur via the class II (noninterfering) pathway, the predicted changes in the CoC were not consistent with observed changes (Figure 2, C and D).

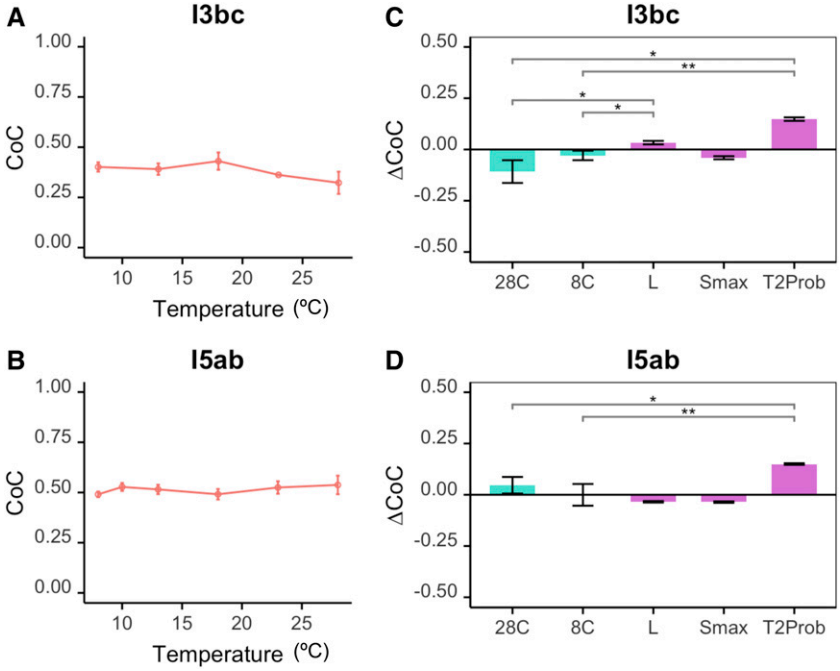

Figure 2 Observed and predicted CoC for intervals I3bc and I5ab. For I3bc (A) and I5ab (B), CoC values were mostly constant across the temperature range, although for I3bc the CoC was slightly lower at 28° than at 18° (P = 0.018; pairwise Student's t-test with Bonferroni correction). (C and D) The change in CoC observed between 18 and 28 or 8° is shown in teal; the change in CoC predicted by changes in a single beam-film model parameter that results in a 13% increase in COs (*i.e.*, the average increase observed at temperature extremes) is shown in purple. Observed changes in CoC are consistent with changes predicted by altering beam-film model parameters that affect class I COs: L and/or Smax. The observed changes in CoC are not consistent with changes predicted by altering the number of class II COs (T2 Prob). Error bars indicate 95% C.I.s. CoC, coefficient of coincidence; L, the proportion of the chromosome over which interference propagates (*i.e.*, the proportion of the chromosome over which stress is relieved); Smax, the crossover designation driving force; T2 Prob, the proportion of potential crossover sites that develop into noninterfering class II crossovers.

Consistent with the hints from the CoC trends, the modeling suggests that increased crossovers observed as temperature changes in *A. thaliana* occur exclusively or primarily via the interference-sensitive class I (ZMM) pathway.

Increased crossovers occur via the class I pathway

To empirically test whether the class I/ZMM-dependent crossovers are indeed responsible for the observed increases in recombination at high or low temperature, we quantified the number of MLH1 foci. MLH1 is a member of the MutL complex together with MLH3 and marks sites of class I crossovers (White *et al.* 2017). We counted MLH1 foci in pachytene nuclei from plants exposed to 8, 18, or 28° for 1 week (Figure 3A). We found a significant increase in MLH1 foci when comparing 18 and 28° (Mann–Whitney U test, P = 0.01681), indicating that high temperature does cause an increase in class I crossovers as predicted by the modeling. However, we did not observe an increase in MLH1 foci at 8° (1 or 6 weeks) compared to 18° (Mann–Whitney U test, P = 0.4299 and P = 0.503, respectively; Figure 3B and Figure S7 in File S1).

While the low-temperature results are at first pass puzzling in the context of modeling predictions, there is some evidence that MLH1-independent class I crossovers can occur in *Arabidopsis*: loss of any of several ZMM proteins (and hence all class I crossovers) result in an 85% reduction in crossovers (*e.g.*, Stern 1926; Wilson 1959), while loss of MLH3, and therefore the functional MutL complex (MLH1/MLH3), results in only a 60% reduction (Jackson *et al.* 2006). Thus, we reasoned that low temperature might increase recombination rate via such MLH1-independent class I crossovers. Therefore, we quantified foci of another class I crossover-associated protein, HEI10 (Figure 3D), at both 8 and 18°. In contrast to MLH1, which is observed from pachytene and only marks sites of future crossovers (White *et al.* 2017), HEI10 foci are observed early in meiotic prophase I and initially mark many precursor sites that are not destined to become crossovers (Chelysheva *et al.* 2012). The number of HEI10 foci then reduces until only sites destined to become crossovers are marked by pachytene (Chelysheva *et al.* 2012). For this reason, we only counted HEI10 foci in late pachytene cells in which all five pairs of chromosomes were completely synapsed, or in early diplotene cells in which the SC is just beginning to dissociate. We found a significant increase in HEI10 foci at 8° relative to 18° (Mann–Whitney U test, P = 0.0001316). We also observed a significant increase in HEI10 foci compared to MLH1 foci at 8° (Mann–Whitney U test, P = 0.01543), although no difference between HEI10 or MLH1 foci was observed at 18° (Mann–Whitney U test, P = 0.7198). In agreement with a higher number of HEI10 foci at 8°, most cells at 8° had 1one or two HEI10 foci that did not colocalize with MLH1 (Figure 3F). Taken together, these results suggest that in *A. thaliana* the increased crossover frequency at both high and low temperatures involves an increase in class I interfering crossovers, though the low- and high-temperature effects are mechanistically at least somewhat distinct.

The class II pathway does not contribute to increased crossovers

Though our modeling suggested that class II crossovers are not likely to be involved in the temperature trends we observed in *A. thaliana*, in yeast, class II crossovers had been previously reported to increase in number with low temperatures in some mutant contexts (Mercier *et al.* 2014). Thus, we also wished to test whether class II crossovers might contribute to the temperature effect on recombination in our study. Since there is no robust cytological marker for noninterfering

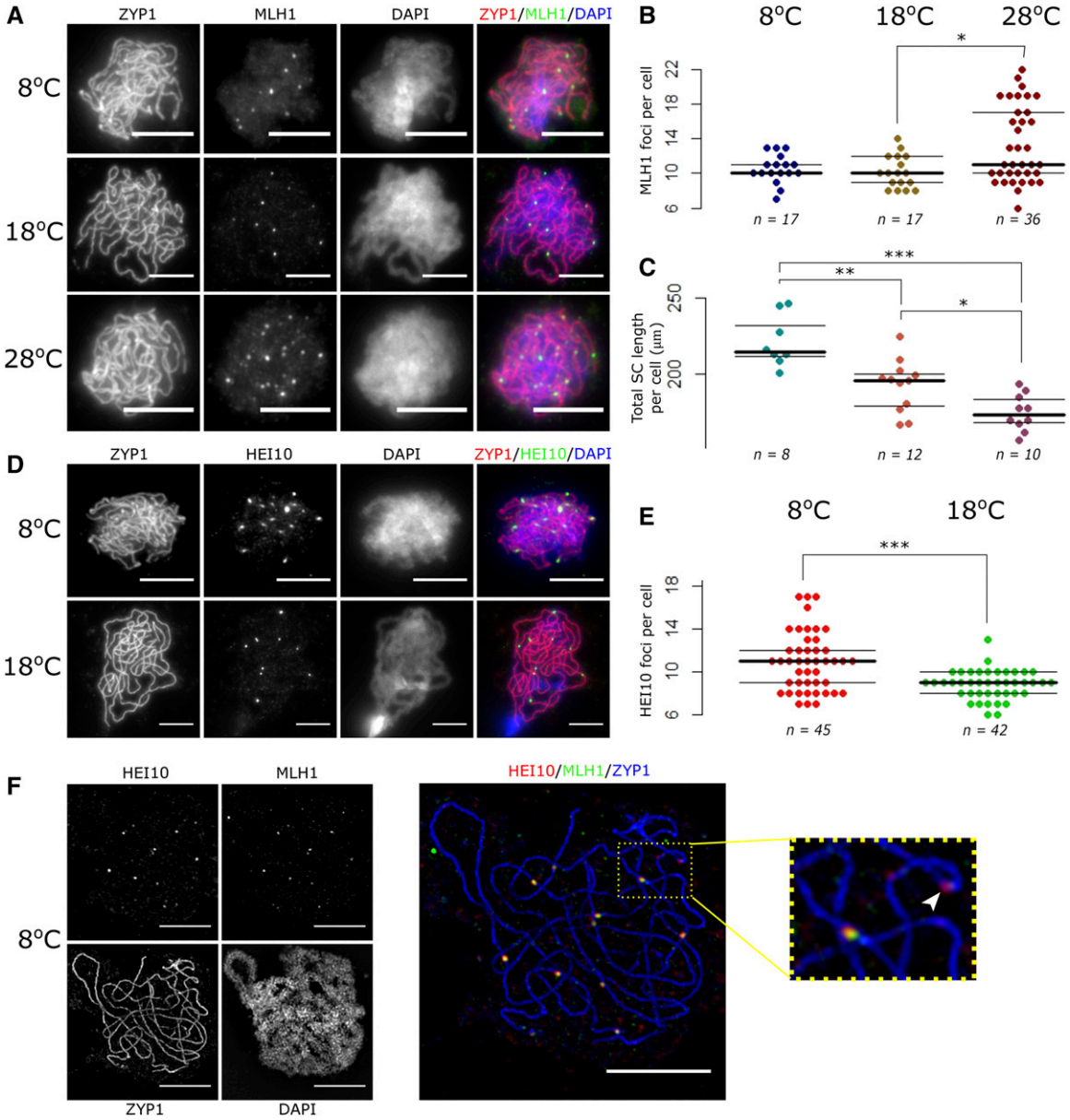

Figure 3 An increase in total class I crossover (CO) frequency is observed at high- and low-temperature extremes and increasing temperature is associated with shorter synaptonemal complex (SC) length. MLH1 foci were counted in pachytene cells stained for ZYP1, MLH1, and DAPI (A) from plants grown for 1 week at 8, 18, and 28°. A plot showing MLH1 foci counts (B) demonstrates a significant increase in total class I CO number at 28° Compared to 18°. Total SC lengths per cell in micrometers (C) also decrease significantly with increasing temperatures. HEI10 foci were also counted in pachytene cells stained for ZYP1, HEI10, and DAPI (D) from plants grown for 1 week at 8 or 18°. A plot showing HEI10 foci counts (E) demonstrates a significant increase in total class I CO number at 8° Compared to 18°. A cell stained for HEI10, MLH1, ZYP1, and DAPI, and imaged using structured-illumination microscopy (F), confirms that additional HEI10 foci are present that are not associated with corresponding MLH1 foci (indicated by arrowhead) in plants grown for 5 weeks at 8°. Bar, 5 μm. * $P < 0.05$, ** $P < 0.005$, and *** $P < 0.0005$.

crossovers in *A. thaliana*, we used recombination assays in mutant lines that lack class I crossovers. First, we repeated the pollen-based recombination assay for FTL line I3bc in a *zip4*, *fancm* double mutant. In *A. thaliana*, *zip4* mutants lack class I crossovers leading to semisterility (Chelysheva *et al.* 2007), while *fancm* mutants have increased class II crossovers (Crismani *et al.* 2012). This increase in crossovers restores pollen viability to the double *zip4*, *fancm* mutant under standard growing conditions (Crismani *et al.* 2012), enabling the pollen-based FTL assay to be used. In the *fancm*, *zip4* background, crossover levels were unchanged at 28° Compared to 18° (Figure S8A in File S1; $P = 0.986$, pairwise Student's *t*-test with Bonferroni correction), confirming that increased recombination at high temperature occurs exclusively or primarily via the class I pathway. Crossover number increased at low temperature with borderline significance (10° *vs.* 18°, $P = 0.058$, pairwise Student's *t*-test with Bonferroni correction, Figure S8A in File S1). However, pollen

viability was also drastically reduced in these double mutants at temperatures below 18°, suggesting that FANCM becomes more important at lower temperatures, at least in the absence of class I crossovers (Figures S8B and S9 in File S1).

While the results for *zip4*, *fancm* double mutants at low temperature might suggest an increase in class II crossovers at low temperatures in *A. thaliana*, similar to that observed at low temperature in yeast *zmm* mutants, we were concerned that: (1) low pollen viability may have introduced a sampling bias in the double mutant at low temperature, or (2) the unanticipated requirement for FANCM at lower temperatures in the absence of class I crossovers may have affected our results in complex ways that are not necessarily relevant in a wild-type context. Therefore, we used a second cytological assay to investigate the effect of low temperature on class II crossovers, performing chiasma counts on metaphase I cells from *msh5* mutants after exposure to either 8 or 18° for 1 week. MSH5, a ZMM protein, is absolutely required for class I crossovers, and the only chiasmata that remain in an *msh5* mutant occur via the class II pathway (Higgins *et al.* 2008b). Unlike FANCM, MSH5 does not affect the class II pathway. We found that in this mutant there was no significant difference in chiasma counts between 8° ($n = 56$ cells, mean chiasma number = 1.44) and 18° ($n = 85$ cells, mean chiasma number = 1.46; χ^2 test, $P = 0.792$; Figure S7 in File S1). Unlike the pollen-based recombination assay we used for the *zip4*, *fancm* double mutants, the metaphase I bivalent counts occur before any potential sampling bias is introduced due to low pollen viability, and therefore likely better represents the effect of temperature on class II crossovers. These results suggest that the number of class II crossovers remains essentially unchanged across the tested temperature range in *A. thaliana*.

SC length is negatively correlated with temperature

A previous study in barley demonstrated that a slightly increased crossover frequency at higher temperatures was associated with a concurrent increase in chromosome length as measured by the length of the SC, suggesting that the longer chromosome length might explain the increase in crossover rate at higher temperatures (Phillips *et al.* 2015). SC length is also known to positively correlate with crossover numbers in mammals (Lynn *et al.* 2002). Therefore, we measured total SC length in our MLH1/ZYP1-stained pachytene cells from *A. thaliana* grown at different temperatures to ask whether the same trend is seen (Figure 3C) (ZYP1 is the synaptonemal central element protein of *A. thaliana*, (Higgins *et al.* 2005). In contrast to barley, we observed that in *A. thaliana* total SC length significantly decreased with increasing temperatures and that this was consistent (a linear decline) across the whole temperature range (Mann–Whitney *U* test, 8° *vs.* 18° $P = 0.001064$, 18° *vs.* 28° $P = 0.0169$, and 8° *vs.* 28° $P = 0.0000457$). Thus, in *A. thaliana*, the increase in crossover number at elevated temperatures cannot be explained by an increase in SC length. However, the low-temperature effect could be; when factoring in the observed 14% (28 ± 8 μm) increase in SC length at 8° relative to 18°, the beam-film model predicts a 16% increase in class I crossovers (or a 14% increase in total recombination). This is consistent with the observed increases in recombination measured by the pollen-based assay (8–18% increase in total recombination) and HEI10 foci counts (14–34% increase in class I crossovers).

Discussion

In this study, we demonstrate that male meiotic recombination rate increases at temperatures both above and below a nadir at 18° in the Col-0 strain of *A. thaliana*. We show that both the high- and low-temperature increases appear to result wholly or mostly from an increase in class I interfering crossovers, but that the high- and low-temperature effects may be mechanistically at least somewhat distinct. The low-temperature increase in HEI10-marked, but MLH1-negative, foci may be explainable by a concomitant increase in axis length of ~14% at lower temperatures. At high temperatures, on the other hand, axis length decreases, and thus cannot explain an increase in MLH1 foci and recombination.

There are reasons to think that the effect of temperature on recombination may be in large part biophysical. For example, the length and integrity of the SC, which is what correlates with recombination rates (Zickler and Kleckner 2015), is known to be affected by temperature (*e.g.*, Phillips *et al.* 2015; Rog *et al.* 2017). The recent observation that the SC displays liquid crystal-like properties (Rog *et al.* 2017) suggests one possible mechanism. Liquid crystal structures could be easily perturbed by temperature, and indeed, extreme temperatures can lead to aberrant SC polymerization into polycomplexes [see Morgan *et al.* (2017)]. But this could also have important implications in understanding how recombination responds to subtler temperature changes, since even minor perturbation in the SC can cause quantitative effects on recombination frequency (Higgins *et al.* 2005). Liquid crystal properties of the SC could also provide a possible explanation for our observation that low temperature may increase the frequency of a specific subset of MLH1-independent, but ZMM-dependent (class I), crossovers. If the SC is less fluid at lower temperature, it may be able to stabilize Holliday junctions without an absolute requirement for the MutL complex.

A variety of stresses other than temperature also affect recombination rates (De Storme and Geelen 2014; Bomblies *et al.* 2015). If we envision the perturbations in meiosis as direct effects of temperature on the relevant proteins, how can these other effects be explained? Stress from a wide range of sources affects the oxidative state of the cell, which can also affect protein function and stability directly. Interestingly, one protein that is known to be very responsive to oxidative state is the cohesin subunit REC8 (Perkins *et al.* 2016), which is important for axis emplacement and recombination (Molnar *et al.* 1995; Bai *et al.* 1999; Cai *et al.* 2003). Cohesin failures can, in turn, mimic temperature-related failures, specifically in the aggregation of axis proteins. These

similarities suggest that cohesin may be a particularly sensitive component of meiosis and that its perturbation can have reverberating effects through the subsequent processes of axis formation and recombination. Other factors may also play a role. It is known, for instance, that abscisic acid signaling and chromatin decondensation increase in response to temperature stress (Pecinka *et al.* 2010; Finkelstein 2013), and both are associated with increased recombination (Yin *et al.* 2009; Henderson 2012).

Our data suggest that temperature affects exclusively or primarily class I interfering crossovers in *A. thaliana*. This is in line with reports in barley that class I crossovers are repositioned under warmer temperatures (Phillips *et al.* 2015). The barley study did not examine class II crossovers, but in yeast, class II crossovers have been reported to increase under temperature stress (Börner *et al.* 2004). This contrasts with our findings in *A. thaliana*, where class II crossovers showed no response to temperature, suggesting that there may be variation among taxa in the sensitivity of particular crossover pathways to temperature. Such variation could result if specific proteins involved in different aspects of meiosis have different thermosensitivities across taxa. In mice and lilies, for example, there is evidence that particular recombinases are directly sensitive to temperature (Hotta *et al.* 1985, 1988; Stern 1986), which may play a role here too. Another possible explanation may be a shift in crossover maturation dynamics. Previous experiments in yeast demonstrated that low temperatures can affect the dynamics of early steps in meiotic recombination (Börner *et al.* 2004), which may cause some crossovers to mature earlier or later at low temperatures, and could affect crossover rates as well as the presence of (or our ability to detect) MLH1 foci at late pachytene. In barley, a change in the dynamics of DNA replication, specifically the replication of heterochromatic DNA, can affect the ultimate positioning of crossover events, though in this species it has negligible effects on their number (Higgins *et al.* 2012). Together with results from yeast, this hints that the timing of different stages of early meiotic events can alter crossover outcomes, though the details of how temperature affects the timing of meiotic events in *A. thaliana* has yet to be described in detail. Another factor may be that the SC is longer at lower temperatures, which could provide more physical space for crossovers to form (*e.g.*, Lynn *et al.* 2002; Phillips *et al.* 2015).

Our results are consistent with the idea that meiotic recombination is tuned to the environment of a given species (Bomblies *et al.* 2015; Wright *et al.* 2015). The change in recombination that occurs under temperature increases or decreases in most species is a plastic response that is either adaptive in itself (Ritz *et al.* 2017) and/or reflects unavoidable instability in the system (Morgan *et al.* 2017). Plasticity of recombination has been previously described in some circumstances as a possibly adaptive response to increase diversity in offspring (Modliszewski and Copenhaver 2015). However, considering how common it is, we favor the idea that recombination rate plasticity, rather than being a directly selected trait, is an unavoidable byproduct of the thermosensitivity of core meiotic proteins and/or processes, and that any benefits that arise from the increase in recombination are inadvertent (Morgan *et al.* 2017). Nevertheless, even if it is just a happy accident, it may well be that increasing recombination under temperature deviations does in fact benefit future generations by facilitating rapid adaptation.

U-shaped curves in response to temperature suggest that in "optimal" conditions, organisms generally have lower recombination rates than under stressful conditions. This is somewhat surprising given that elevated recombination rates may be advantageous for adaptation in at least some circumstances (*e.g.*, Barton 1995; Charlesworth and Barton 1996; Presgraves 2005; Otto 2009; Campos *et al.* 2015). Indeed, numerous empirical studies have shown that strong artificial selection for a wide variety of traits is correlated with an increase in recombination rates (*e.g.*, Flexon and Rodell 1982; Korol and Iliadi 1994; Ross-Ibarra 2004). However, a potential explanation for why there might be a low point in recombination is that in a stable environment to which an organism is well adapted, minimizing recombination (while still ensuring at least one crossover per bivalent) better maintains allelic combinations that have been selected in previous generations (Otto 2009). An additional possibility is that recombination, while important for chromosome segregation in most species, is also mutagenic, and thus may be selected against (Arbeithuber *et al.* 2015). Moreover, there is an important exception to the aforementioned trend that selection tends to increase recombination. For example, when selection is applied for high fertility in mice, recombination rates decline, suggesting that high recombination can decrease fertility and may thus be evolutionarily selected against (Gorlov *et al.* 1992), even if no obvious immediate defects are observed with even very high recombination rates (Girard *et al.* 2014).

There is evidence from several species that recombination rate may be linked with local adaptation. For example, in grasshoppers, individuals with lower crossover rates are more sensitive to temperature shock (Rees and Thompson 1958; Shaw 1971), while wild *Sordaria* growing in distinct habitats have different recombination rates when grown together in laboratory conditions (Saleem *et al.* 2001). There is also evidence that natural selection has acted in populations adapted to different habitats on core meiotic proteins that have the potential to affect recombination rates (Turner *et al.* 2008; Anderson *et al.* 2009; Wright *et al.* 2015). The notion that temperature affects recombination and that populations adapt to local prevailing climates has important implications for interpreting observations of recombination rate variation among populations when these are measured at a single temperature in the lab. It may be, in at least some cases, that as populations adapt to distinct environments, the recombination response curves shift in concert. If this is the case, when measuring recombination rate at a single laboratory temperature, we may be sampling different points on a given genotype's response curve, which may not be reflective of what occurs in nature. For these reasons, it will be important to

better understand both the causes and the consequences of the links between stress, temperature, and meiotic recombination (Bomblies *et al.* 2015) both from a mechanistic and evolutionary perspective.

Acknowledgments

We thank Eric Jenczewski for discussion of the manuscript, Mathilde Grelon and Ian Henderson for provision of the seeds for the FTL lines, and Gregory Copenhaver who developed these lines. This work was supported by a European Research Council Consolidator grant to K.B. (CoG EVO-MEIO 681946), a Marie Curie fellowship to A.L. (PIOF-GA-2013- 628128), and a UK Biological and Biotechnology Research Council (BBSRC) studentship to C.M. (DTP BB/MO1116 x/1 M1BTP). This work has also been supported by the BBSRC via grant BB/P013511/1 to the John Innes Centre.

Literature Cited

Anderson, J. A., W. D. Gilliland, and C. H. Langley, 2009 Molecular population genetics and evolution of *Drosophila* meiosis genes. Genetics 181: 177–185. https://doi.org/10.1534/genetics.108.093807

Arbeithuber, B., A. J. Betancourt, T. Ebner, and I. Tiemann-Boege, 2015 Crossovers are associated with mutation and biased gene conversion at recombination hotspots. Proc. Natl. Acad. Sci. USA 112: 2109–2114. https://doi.org/10.1073/pnas.1416622112

Armstrong, S. J., A. P. Caryl, G. H. Jones, and F. C. H. Franklin, 2002 Asy1, a protein required for meiotic chromosome synapsis, localizes to axis-associated chromatin in Arabidopsis and Brassica. J. Cell Sci. 115: 3645–3655. https://doi.org/10.1242/jcs.00048

Armstrong, S. J., F. C. H. Franklin, and G. H. Jones, 2003 A meiotic timecourse for *Arabidopsis thaliana*. Sex. Plant Reprod. 16: 141–149. https://doi.org/10.1007/s00497-003-0186-4

Bai, X., B. N. Peirson, F. Dong, C. Xue, and C. A. Makaroff, 1999 Isolation and characterization of SYN1, a RAD21-like gene essential for meiosis in *Arabidopsis*. Plant Cell 11: 417–430. https://doi.org/10.1105/tpc.11.3.417

Barton, N. H., 1995 A general model for the evolution of recombination. Genet. Res. 65: 123–144. https://doi.org/10.1017/S0016672300033140

Basu-Roy, S., F. Gauthier, L. Giraut, and C. Mézard, 2013 Hot regions of noninterfering crossovers coexist with a nonuniformly interfering pathway in *Arabidopsis thaliana*. Genetics 195: 769–779. https://doi.org/10.1534/genetics.113.155549

Berchowitz, L. E., and G. P. Copenhaver, 2010 Genetic interference: don't stand so close to me. Curr. Genomics 11: 91–102. https://doi.org/10.2174/138920210790886835

Berchowitz, L. E., K. E. Francis, A. L. Bey, and G. P. Copenhaver, 2007 The role of AtMUS81 in interference-insensitive crossovers in *A. thaliana*. PLoS Genet. 3: e132. https://doi.org/10.1371/journal.pgen.0030132

Bilgir, C., C. R. Dombecki, P. F. Chen, A. M. Villeneuve, and K. Nabeshima, 2013 Assembly of the synaptonemal complex is a highly temperature-sensitive process that is supported by PGL-1 during *Caenorhabditis elegans* meiosis. G3 (Bethesda) 3: 585–595. https://doi.org/10.1534/g3.112.005165

Bomblies, K., J. D. Higgins, and L. Yant, 2015 Meiosis evolves: adaptation to external and internal environments. New Phytol. 208: 306–323. https://doi.org/10.1111/nph.13499

Börner, G. V., N. Kleckner, and N. Hunter, 2004 Crossover/noncrossover differentiation, synaptonemal complex formation, and regulatory surveillance at the leptotene/zygotene transition of meiosis. Cell 117: 29–45. https://doi.org/10.1016/S0092-8674(04)00292-2

Cai, X., F. Dong, R. E. Edelmann, and C. Makaroff, 2003 The Arabidopsis SYN1 cohesin protein is required for sister chromatid arm cohesion and homologous chromosome pairing. J. Cell Sci. 116: 2999–3007. https://doi.org/10.1242/jcs.00601

Campos, L., D. L. Halligan, P. R. Haddrill, and B. Charlesworth, 2015 The relation between recombination rate and patterns of molecular evolution and variation in *Drosophila melanogaster*. Mol. Biol. Evol. 31: 1010–1028. https://doi.org/10.1093/molbev/msu056

Caryl, A. P., S. J. Armstrong, G. H. Jones, and F. C. H. Franklin, 2000 A homologue of the yeast HOP1 gene is inactivated in the Arabidopsis meiotic mutant asy1. Chromosoma 109: 62–71. https://doi.org/10.1007/s004120050413

Charlesworth, B., and N. H. Barton, 1996 Recombination load associated with selection for increased recombination. Genet. Res. 67: 27–41. https://doi.org/10.1017/S0016672300033450

Chelysheva, L., G. Gendrot, D. Vezon, M.-P. Doutriaux, R. Mercier *et al.*, 2007 Zip4/Spo22 is required for class I CO formation but not for synapsis completion in *Arabidopsis thaliana*. PLoS Genet. 3: e83. https://doi.org/10.1371/journal.pgen.0030083

Chelysheva, L., D. Vezon, A. Chambon, G. Gendrot, L. Pereira *et al.*, 2012 The *Arabidopsis* HEI10 is a new ZMM protein related to Zip3. PLoS Genet. 8: e1002799. https://doi.org/10.1371/journal.pgen.1002799

Crismani, W., C. Girard, N. Froger, M. Padrillo, J. L. Santos *et al.*, 2012 FANCM limits meiotic crossovers. Science 336: 1588–1590. https://doi.org/10.1126/science.1220381

De Storme, N., and D. Geelen, 2014 The impact of environmental stress on male reproductive development in plants: biological processes and molecular mechanisms. Plant Cell Environ. 37: 1–18. https://doi.org/10.1111/pce.12142

De Storme, N., G. P. Copenhaver, and D. Geelen, 2012 Production of diploid male gametes in *Arabidopsis* by cold-induced destabilization of post-meiotic radial microtubule arrays. Plant Physiol. 160: 1808–1826. https://doi.org/10.1104/pp.112.208611

Elliott, C. G., 1955 The effect of temperature on chiasma frequency. Heredity 9: 385–398. https://doi.org/10.1038/hdy.1955.39

Finkelstein, R., 2013 Abscisic acid synthesis and response. Arabidopsis Book 11: e0166. https://doi.org/10.1199/tab.0166

Flexon, P. B., and C. F. Rodell, 1982 Genetic recombination and directional selection for DDT resistance in *Drosophila melanogaster*. Nature 298: 672–674. https://doi.org/10.1038/298672a0

Francis, K. E., S. Y. Lam, B. D. Harrison, A. L. Bey, L. E. Berchowitz *et al.*, 2007 Pollen tetrad-based visual assay for meiotic recombination in Arabidopsis. Proc. Natl. Acad. Sci. USA 104: 3913–3918. https://doi.org/10.1073/pnas.0608936104

Girard, C., W. Crismani, N. Froger, J. Mazel, A. Lemhemdi *et al.*, 2014 FANCM-associated proteins MHF1 and MHF2, but not the other Fanconi anemia factors, limit meiotic crossovers. Nucleic Acids Res. 42: 9087–9095. https://doi.org/10.1093/nar/gku614

Gorlov, I., L. Schuler, L. Bunger, and P. Borodin, 1992 Chiasma frequency in strains of mice selected for litter size and for high body weight. Theor. Appl. Genet. 84: 640–642.

Henderson, I. R., 2012 Control of meiotic recombination frequency in plant genomes. Curr. Opin. Plant Biol. 15: 556–561. https://doi.org/10.1016/j.pbi.2012.09.002

Higgins, J. D., E. Sanchez-Moran, S. J. Armstrong, G. H. Jones, and F. C. H. Franklin, 2005 The Arabidopsis synaptonemal complex protein ZYP1 is required for chromosome synapsis and

normal fidelity of crossing over. Genes Dev. 19: 2488–2500. https://doi.org/10.1101/gad.354705

Higgins, J. D., E. F. Buckling, F. C. H. Franklin, and G. H. Jones, 2008a Expression and functional analysis of AtMUS81 in *Arabidopsis* meiosis reveals a role in the second pathway of crossing-over. Plant J. 54: 152–162. https://doi.org/10.1111/j.1365-313X.2008.03403.x

Higgins, J. D., J. Vignard, R. Mercier, A. G. Pugh, and G. H. Jones, 2008b AtMSH5 partners AtMSH4 in the class I meiotic cross-over pathway in *Arabidopsis thaliana*, but is not required for synapsis. Plant J. 55: 28–39. https://doi.org/10.1111/j.1365-313X.2008.03470.x

Higgins, J. D., R. M. Perry, A. Barakate, L. Ramsey, R. Waugh *et al.*, 2012 Spatiotemporal asymmetry of the meiotic program underlies the predominantly distal distribution of meiotic crossovers in barley. Plant Cell 24: 4096–4109. https://doi.org/10.1105/tpc.112.102483

Hotta, Y., S. Tabata, R. A. Bouchard, R. Piñon, and H. Stern, 1985 General recombination mechanisms in extracts of meiotic cells. Chromosoma 93: 140–151. https://doi.org/10.1007/BF00293161

Hotta, Y., M. Fujisawa, S. Tabata, H. Stern, and S. Yoshida, 1988 The effect of temperature on recombination activity in testes of rodents. Exp. Cell Res. 178: 163–168. https://doi.org/10.1016/0014-4827(88)90387-4

Jackson, N., E. Sanchez-Moran, E. Buckling, S. J. Armstrong, G. H. Jones *et al.*, 2006 Reduced meiotic crossovers and delayed prophase I progression in AtMLH3-deficient *Arabidopsis*. EMBO J. 25: 1315–1323. https://doi.org/10.1038/sj.emboj.7600992

Jensen, J., 1981 Effect of temperature on genetic recombination in barley. Hereditas 94: 215–218. https://doi.org/10.1111/j.1601-5223.1981.tb01755.x

Korol, A. B., and K. G. Iliadi, 1994 Increased recombination frequencies resulting from directional selection for geotaxis in *Drosophila*. Heredity 72: 64–68. https://doi.org/10.1038/hdy.1994.7

Lambing, C., K. Osman, K. Nuntasoontorn, A. West, J. D. Higgins *et al.*, 2015 Arabidopsis PCH2 mediates meiotic chromosome remodeling and maturation of crossovers. PLoS Genet. 11: e1005372. https://doi.org/10.1371/journal.pgen.1005372

Longair, M. H., D. A. Baker, and J. D. Armstrong, 2011 Simple neurite tracer: open source software for reconstruction, visualization and analysis of neuronal processes. Bioinformatics 27: 2453–2454. https://doi.org/10.1093/bioinformatics/btr390

Lynn, A., K. E. Koehler, L. Judis, E. R. Chan, J. P. Cherry *et al.*, 2002 Covariation of synaptonemal complex length and mammalian meiotic exchange rates. Science 296: 2222–2225. https://doi.org/10.1126/science.1071220

Lynn, A., R. Soucek, and G. V. Börner, 2007 ZMM proteins during meiosis: crossover artists at work. Chromosome Res. 15: 591–605. https://doi.org/10.1007/s10577-007-1150-1

Mercier, R., S. Jolivet, D. Vezon, E. Huppe, L. Chelysheva *et al.*, 2005 Two meiotic crossover classes cohabit in *Arabidopsis*: one is dependent on MER3, whereas the other one is not. Curr. Biol. 15: 692–701. https://doi.org/10.1016/j.cub.2005.02.056

Mercier, R., C. Mezard, E. Jenczewski, N. Macaisne, and M. Grelon, 2014 The molecular biology of meiosis in plants. Annu. Rev. Plant Biol. 66: 1–31.

Modliszewski, J. L., and G. P. Copenhaver, 2015 Meiotic recombination heats up. New Phytol. 208: 295–297. https://doi.org/10.1111/nph.13618

Molnar, M., J. Bahler, M. Sipiczki, and J. Kohli, 1995 The rec8 gene of *Schizosaccharomyces pombe* is involved in linear element formation, chromosome pairing and sister-chromatid cohesion during meiosis. Genetics 141: 61–73.

Morgan, C. H., H. Zhang, and K. Bomblies, 2017 Are the effects of elevated temperature on meiotic recombination and thermotolerance linked via the axis and synaptonemal complex? Philos. Trans. R. Soc. Lond. B Biol. Sci. 372: 20160470. https://doi.org/10.1098/rstb.2016.0470

Otto, S., 2009 The evolutionary enigma of sex. Am. Nat. 174: S1–S14. https://doi.org/10.1086/599084

Pecinka, A., H. Q. Dinh, T. Baubec, M. Rosa, N. Lettner *et al.*, 2010 Epigenetic regulation of repetitive elements is attenuated by prolonged heat stress in *Arabidopsis*. Plant Cell 22: 3118–3129. https://doi.org/10.1105/tpc.110.078493

Perkins, A. T., T. M. Das, L. C. Panzera, and S. E. Bickel, 2016 Oxidative stress in oocytes during midprophase induces premature loss of cohesion and chromosome segregation errors. Proc. Natl. Acad. Sci. USA 113: E6823–E6830. https://doi.org/10.1073/pnas.1612047113

Phillips, D., G. Jenkins, M. Macaulay, C. Nibau, J. Wnetrzak *et al.*, 2015 The effect of temperature on the male and female recombination landscape of barley. New Phytol. 208: 421–429. https://doi.org/10.1111/nph.13548

Plough, H. H., 1917 The effect of temperature on crossingover in Drosophila. J. Exp. Zool. 24: 147–209. https://doi.org/10.1002/jez.1400240202

Presgraves, D. C., 2005 Recombination enhances protein adaptation in *Drosophila melanogaster*. Curr. Biol. 15: 1651–1656. https://doi.org/10.1016/j.cub.2005.07.065

Rees, H., and J. Thompson, 1958 Genotypic control of chromosome behaviour in rye. V. The distribution pattern of chiasmata between pollen mother cells. Heredity 12: 101–111. https://doi.org/10.1038/hdy.1958.8

Ritz, K. R., M. A. F. Noor, and N. D. Singh, 2017 Variation in recombination rate: adaptive or not? Trends Genet. 33: 364–374. https://doi.org/10.1016/j.tig.2017.03.003

Rog, O., S. Kohler, and A. F. Dernburg, 2017 The synaptonemal complex has liquid crystalline properties and spatially regulates meiotic recombination factors. Elife 6: e21455. https://doi.org/10.7554/eLife.21455

Ross-Ibarra, J., 2004 The evolution of recombination under domestication: a test of two hypotheses. Am. Nat. 163: 105–112. https://doi.org/10.1086/380606

Saleem, M., B. Lamb, and E. Nevo, 2001 Inherited differences in crossing over and gene conversion frequencies between wild strains of *Sordaria fimicola* from "Evolution Canyon." Genetics 159: 1573–1593.

Shaw, D., 1971 Genetic and environmental components of chiasma control. I. Spatial and temporal variation in *Schistocerca* and *Stethophyma*. Chromosoma 34: 281–301. https://doi.org/10.1007/BF00286154

Smith, H. F., 1936 Influence of temperature on crossing-over in Drosophila. Nature 138: 329–330. https://doi.org/10.1038/138329b0

Stern, C., 1926 An effect of temperature and age on crossing-over in the first chromosome of *Drosophila melanogaster*. Proc. Natl. Acad. Sci. USA 12: 530–532. https://doi.org/10.1073/pnas.12.8.530

Stern, H., 1986 Meiosis: some considerations. J. Cell Sci. Suppl. 4: 29–43. https://doi.org/10.1242/jcs.1986.Supplement_4.3

Turner, T. L., M. T. Levine, M. L. Eckert, and D. J. Begun, 2008 Genomic analysis of adaptive differentiation in *Drosophila melanogaster*. Genetics 179: 455–473. https://doi.org/10.1534/genetics.107.083659

White, M. A., S. Wang, L. Zhang, and N. Kleckner, 2017 Quantitative modeling and automated analysis of meiotic recombination, pp. 305–323 in *Meiosis*, edited by D. T. Stuart. Springer, New York. https://doi.org/10.1007/978-1-4939-6340-9_18

Wilson, J. Y., 1959 Chiasma frequency in relation to temperature. Genetica 29: 290–303. https://doi.org/10.1007/BF01535715

Wright, K. M., B. Arnold, K. Xue, M. Šurinová, J. O'Connell *et al.*, 2015 Selection on meiosis genes in diploid and tetraploid *Arabidopsis arenosa*. Mol. Biol. Evol. 32: 944–955. https://doi.org/10.1093/molbev/msu398

Yelina, N. E., P. A. Ziolkowski, N. Miller, X. Zhao, K. A. Kelly *et al.*, 2013 High-throughput analysis of meiotic crossover frequency and interference via flow cytometry of fluorescent pollen in *Arabidopsis thaliana*. Nat. Protoc. 8: 2119–2134. https://doi.org/10.1038/nprot.2013.131

Yin, H., X. Zhang, J. Liu, Y. Wang, J. He *et al.*, 2009 Epigenetic regulation, somatic homologous recombination, and abscisic acid signaling are influenced by DNA polymerase epsilon mutation in *Arabidopsis*. Plant Cell 21: 386–402. https://doi.org/10.1105/tpc.108.061549

Zhang, L., Z. Liang, J. Hutchinson, and N. Kleckner, 2014 Crossover patterning by the beam-film model: analysis and implications. PLoS Genet. 10: e1004042. https://doi.org/10.1371/journal.pgen.1004042

Zickler, D., and N. Kleckner, 1999 Meiotic chromosomes: integrating structure and function. Annu. Rev. Genet. 33: 603–754. https://doi.org/10.1146/annurev.genet.33.1.603

Zickler, D., and N. Kleckner, 2015 Recombination, pairing, and synapsis of homologs during meiosis. Cold Spring Harb. Perspect. Biol. 7: a016626. https://doi.org/10.1101/cshperspect.a016626

Ziolkowski, P. A., C. J. Underwood, C. Lambing, M. Martinez-Garcia, E. J. Lawrence *et al.*, 2017 Natural variation and dosage of the HEI10 meiotic E3 ligase control *Arabidopsis* crossover recombination. Genes Dev. 31: 306–317. https://doi.org/10.1101/gad.295501.116

Communicating editor: S. Wright